



Regions and Sub-regions Dysfunctions in Alzheimer's during Rest

K. C. Usha^{1*} and Dr. H. N. Suma²

¹*Department of Electronics and Communication Engineering, BMS College of Engineering, Karnataka, India.*

²*Department of Medical Electronics, BMS College of Engineering, Karnataka, India.*

Authors' contributions

This work was carried out in collaboration among both authors. Preparation of the data acquired from ADNI. Author KCU did the data analysis, components extraction, statistical analysis, interpreting the results and drafting the manuscript. Author HNS did the revision of the manuscript and technical guidance throughout the analysis. Both authors read and approved the final manuscript.

Article Information

DOI: 10.9734/AJMAH/2020/v18i530205

Editor(s):

(1) Dr. Janvier Gasana, Kuwait University, Kuwait.

Reviewers:

(1) S. Danish Kadir, University of Rajshahi, Bangladesh.

(2) Ana Paula Dalmagro, Universidade do Vale do Itajaí, Brazil.

(3) Bruno Bastos Godoi, Federal University of Jequitinhonha's Valley and Mucuri, Brazil.

Complete Peer review History: <http://www.sdiarticle4.com/review-history/57122>

Original Research Article

Received 26 March 2020

Accepted 03 June 2020

Published 16 June 2020

ABSTRACT

Aims: Alterations in the cerebrum structurally and functionally are triggered largely due to an increase in neuro depressive brain disorders like Alzheimer's. This study aims is to determine these alterations in the regions of the cerebrum which are significant and distinguishing in Alzheimer's disease subjects compared to healthy. We employ the most potential resting-state functional Magnetic Resonance Imaging (rs-fMRI) modality for this analysis.

Methodology: 24 Alzheimer's disease (AD) and 25 Healthy Controlled (HC) subjects were evaluated with rs-fMRI which is more efficient in anticipating neuronal activity changes. Thus, obtained data of all subjects were preprocessed and components of larger networks to smaller regions were extracted by independent component analysis (ICA) method. Differences in resting-state connectivity were examined for 6 networks of interest viz., Auditory network, Central Executive network, Default mode network, Silence mode network, Sensory-motor network and Visual network and their regions, which are affected due to the common symptoms of Alzheimer's

*Corresponding author: E-mail: ushagautamsk@gmail.com;

disease-like memory, thinking and behavioral changes. Statistical analysis was done with one sample t-test to check the functional connectivity activations in Resting-State Networks (RSNs) and regions of both AD & HC groups at a threshold of $T > 2$. Finally, to obtain the abnormal sub-regions in each of the RSNs of AD a two-sample t-test was carried out at a threshold of $P < .03$.

Results: Our method potentially identifies the functional connectivity alterations and core regions dysfunction amongst the major 6 RSNs in AD compared to HC subjects. The results also showed decreased connectivity in regions of sensory-motor and default mode networks increased connectivity in regions of central executive and silence mode network along with some of the sub-regions dysfunctions in AD.

Conclusion: Modifications in functional connectivity within the major RSNs and regions have been detected which serves as a capability to determine an early biomarker and examining the disease progression.

Keywords: Functional Magnetic Resonance Imaging (fMRI); resting-state fMRI; functional connectivity; Alzheimer's disease; independent component analysis; resting state networks; auditory network; central executive network; default mode network; salience network; sensory-motor network; visual network.

ABBREVIATIONS

AD : Alzheimer's disease;
ADNI : Alzheimer's disease Neuroimaging Initiative;
BOLD : Blood oxygen level dependent;
fALFF : Fractional amplitude of low frequency fluctuations
fMRI : Functional magnetic resonance imaging;
RS-fMRI : Resting state fMRI;
RSN : Resting state networks;
ICA : Independent components analysis;
GIFT : Group ICA fMRI toolbox;
DPARSF : Data processing assistance for resting-state fMRI toolbox;

1. INTRODUCTION

The chronic Alzheimer's disease (AD) gradually increases with episodic cognitive decline and progress towards irreparable memory loss, executive functions, language, visuospatial functions, and other behavioral domains. Neuronal dysfunction in AD is mainly due to the role of b-amyloid and neurofibrillary tangles which not only contribute to the structural changes but also functional connectivity deterioration in the brain. Evaluation of these reductions in functional neuronal activity is a sensitive biomarker for AD [1].

Functional magnetic resonance imaging (fMRI) has become increasingly prominent in understanding neuronal activity, which would be significantly widened to explore the functional neuronal network alterations of AD in comparison

with Healthy controlled (HC) subjects. Resting-state functional magnetic resonance imaging (rs-fMRI) is more effective over task-based fMRI. In rs-fMRI the subjects are not given any task, thus excluding the cofounds of task difficulties and allow a review of neural activity when the subjects are at rest and offer valuable functional mapping measure that synchronizes activations between regions that are spatially distinct. Even during the resting period, it has been observed that some of the brain networks are functionally active [2,3], and thus using rs-fMRI modality it has been effective in identifying altered neural connectivity in AD [4].

The neural connectivity in the cortical brain is studied using methods such as Voxel-based [5], the region of interest (ROI) or seed-based analysis [6], graph theory [7], Independent component analysis (ICA) [8] and machine learning methods [9,10]. Independent component analysis (ICA), is the most popular and effective data-driven approach in the analysis of fMRI data. ICA is powerful to disintegrate heterogeneous magnetic resonance signal patterns and identify the resting-state networks (RSNs) from rs-fMRI [11,12]. It is also advantageous compared to other methods since it does not require prior and outside knowledge like ROI or seed-based analysis [13] or parameter and measure selections as in graph theory analysis and it can be used in complementary with machine-learning [14].

The challenging issue faced in ICA analysis is the number of components selection, previous studies have used lower-order components

extraction between 20 to 40 which would lead to the overlapping of the resting-state networks regions and high order components between 70 to 90 and more would lead to over splitting of components [15,16]. In this current work, we set the components to be extracted from a lower-order ranging from 20 components to a higher-order component of 60 in steps of 10, Hence the major network and their regions are addressed. Another major issue is the separation of resting-state components and the artifacts components. Most of the previous studies have explored on an automated method for identification of only language network component [17], hand classification of noise components in single subject [18], SVM classifier [19] and Naive-Bayes algorithm [20] for noise components classification and some have used predefined spatial masks provided by Dante Mantini from Leuven Medical School [8] for classification. In this study we use a simple and efficient method in the identification of valid components by creating the masks with specific regions of interest so, that redundant regions are eliminated. The obtained resting-state components are the measure of functional connectivity within specific brain networks and show optimistic biomarkers in AD studies and helps in exploring abnormal regions in diseased [11].

2. METHODOLOGY

2.1 Participant's

The experimental data is obtained by the publically available dataset ADNI "Alzheimer's Disease Neuroimaging Initiative". It is a non-profitable organization since 2003 which consists of structural and functional magnetic resonance imaging along with positron emission tomography data of Alzheimer's, Mild Cognitive Impairment and normal subjects with detailed basic and clinical information [21].

In this analysis, we make use of the functional MRI and structural MRI data of 49 subjects including 24 AD patients and 25 HC in the database of ADNI-2. AD subjects had MMSE (Mini-Mental State Examination) score between 20-25; CDR (Clinical Dementia Rate) equal to 0.5 or 1 and HC had an MMSE score between 27-30; CDR equal to 0. We excluding the subjects with their head translation exceeding ± 1.5 mm and rotation exceeding ± 1.5 mm. Finally remained with 45 subjects and their details are as shown in Table 1.

Table 1. The participants information

Project	AD	HC
No of subjects	23	22
Gender (male/female)	10/13	7/15
Age	69.3 \pm 6	70.3 \pm 3
MMSE	20-25	27-30
CDR	0.5 or 1	0

2.2 Resting-state Data Collection

The images were obtained from a 3.0 Tesla Philips MRI scanner. Acquisition parameter includes 140 time points, TR=3000 ms, TE=30 ms, flip angle=80°, 48 slices with a thickness of 3.3 mm and spatial resolution of 3 \times 3 \times 3 mm³ and matrix 64 \times 64 as obtained from the database.

2.3 Data Preprocessing

The preprocessing was carried out with DPARSF "Data Processing Assistance for Resting-State fMRI" software tool [22], based on SPM "Statistical Parameter Mapping" in MATLAB and further statistical analysis was done with REST Resting-state fMRI toolkit. The raw data obtained from the ADNI-2 was processed by DPARSF with following steps,

1. Conversion from Digital Imaging and Communications in Medicine (DICOM) format to NIFTI format.
2. Reorientation of both functional and structural data for an alignment check.
3. To reduce the error caused by the subject's adaptation to the circumstances initial 10-time points of the functional images were discarded.
4. Slice timing correction was performed with reference to the last slice.
5. For head movement compensation the images were realigned using a six-parameter rigid-body spatial transformation since excessive head motion may induce large artifacts in fMRI time series.
6. T1 structural images were co-registered to the mean rsfMRI images.
7. Normalization of the images to Standard EPI temple in SPM.
8. Spatial smoothing of functional images with Gaussian kernel 6 mm full width at half maximum filter to reduce white noise and residual effect.
9. Finally, linear drifts are removed and temporal filtering (0.01 Hz~0.08 Hz) were performed.

2.4 Independent Component Analysis

The independent component analysis (ICA) is accomplished using GIFT "Group ICA for fMRI toolbox". After the initial preprocessing ICA separates the fMRI signal into different sources of variance and extracts the spatially independent components. The ICA process includes reduction of subject's functional data dimension using principle component analysis PCA along with INFOMAX algorithm, stable components were obtained by running the analysis 100 times using ICASSO toolbox [23] [24]. The number of components to be extracted is evaluated using Minimum Distance Length (MDL) [25] principle from all participants, the optimal number of components obtained were 60 components; it always varies on the dataset selected. We repeat the ICA, by setting the number of components (ICs) to be extracted from a lower order of 20 signifying larger networks to higher order 60 components signifying smaller regions in steps of 10. Once all the components are extracted next we have to classify the valid components and artifacts. With the sole purpose to examine all the resting-state networks and their regions contributing to the differences in AD progression compared to HC. The subsequent components extracted from both AD and HC include time courses and their respective spatial maps, where the time courses of components representing the brain activity and spatial maps indicating their intensity.

2.5 Identification of RSNs

The extracted components are the combination of resting-state networks with valid brain signals and artifact components due to several causes such as white matter, blood vessels and cerebral fluid. Classification was performed by sorting of components using spatial correlation method. The sorting was carried out using masks created by WFU Pick Atlas [26] software by manually including specific region of interest in the grey matter. The masks with six major resting-state networks and the sub-masks with of all the regions were created. This method of mask creation helped eliminate all the redundant regions resulted from overlap of white matter, cerebrospinal fluid or brain boundaries. After sorting the components with largest correlation values were selected and examined for adequate dynamic range i.e. difference between the peak power and minimum power at frequencies to the right of the peak, fALFF (fractional amplitude of low frequency fluctuations) the integral of

spectral power below 0.10 Hz to the integral of power between 0.15 and 0.25 Hz and finally visually inspected [27]. Hence the components extracted range from lower order comprising of larger networks and higher-order comparing of smaller regions of the networks. The six resting-state network and their region representing the components are auditory network (AN) which includes right and left superior temporal lobe [28], the central executive network (CEN) including right and left regions of dorsolateral prefrontal cortex and posterior parietal cortex, Default mode network (DMN) is consists of medial pre-frontal cortex, inferior parietal lobe, posterior cingulated cortex, precuneus and hippocampus, Salience mode network (SN) includes anterior cingulated cortex and anterior insular [29], sensory-motor network (SMN) which includes precentral and post-central gyrus [30], and visual network (VN) including high and prim visual regions which are the part of the occipital cortex [31].

2.6 Statistical Analysis

The six RSNs and their region components of AD and HC are evaluated for one sample t-test to know the activated brain network regions in each group and to obtain the significant group differences, with results displayed at the threshold of $T > 2$. Finally, the Z-shift was performed. Then two-sample t-tests were accomplished using REST toolbox on the specific region of interest. The masks with region of interest were obtained by the union of activated brain regions of both groups. This estimates the alterations in the functional connectivity of all the networks and regions. Finally results obtained were z transformed and represented with $P < 0.03$ (AlphaSim correction) [8].

3. RESULTS

3.1 Spatial Distribution in RSNs

One-sample t-test ($T > 2$) results depict the resting-state network in two groups have typical spatial distribution patterns. The differences in spatial pattern distribution of auditory, central executive, default, salience, sensory-motor and visual networks along with their regions are as shown in Figs. 1-4 below. The auditory, sensory-motor and visual being sensory networks show decreased functional connectivity in AD; executive and salience network part of the attention networks show increased

connectivity and default mode network which are active when the subjects are at rest, shows reduced connectivity in AD as compared to HC [32,33].

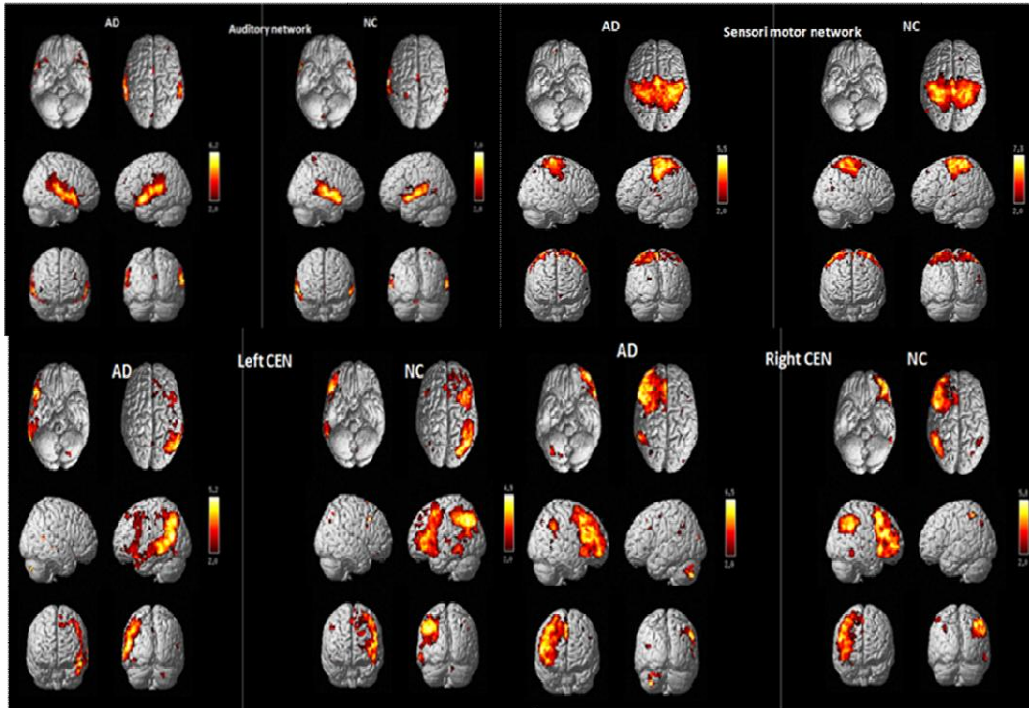


Fig. 1. Auditory, sensory-motor and executive network functional activations differences in AD and HC

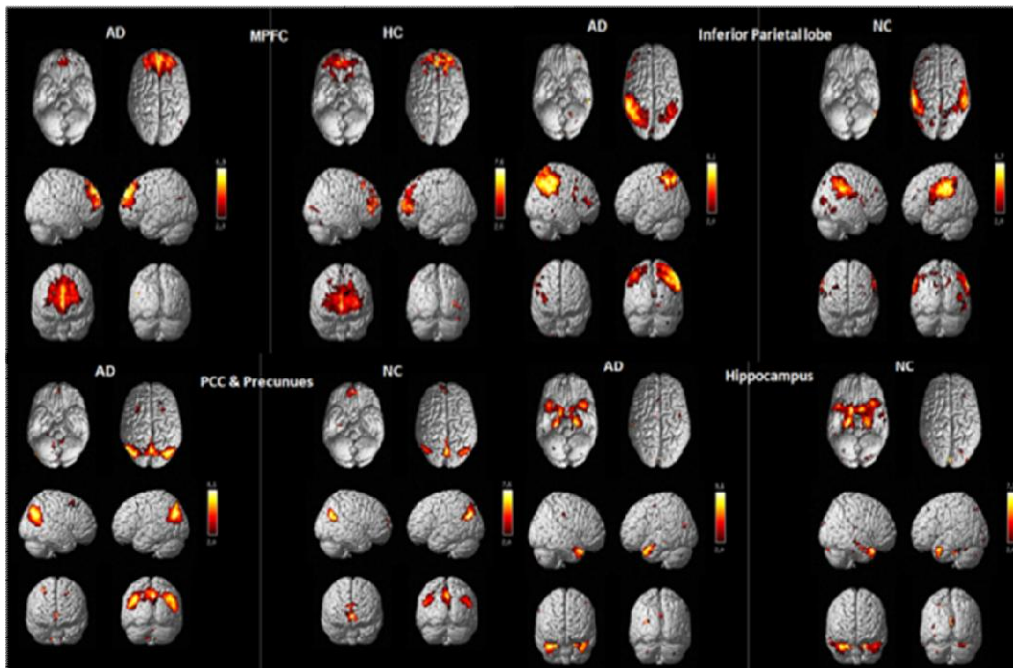


Fig. 2. Default mode network functional activation differences in AD and HC

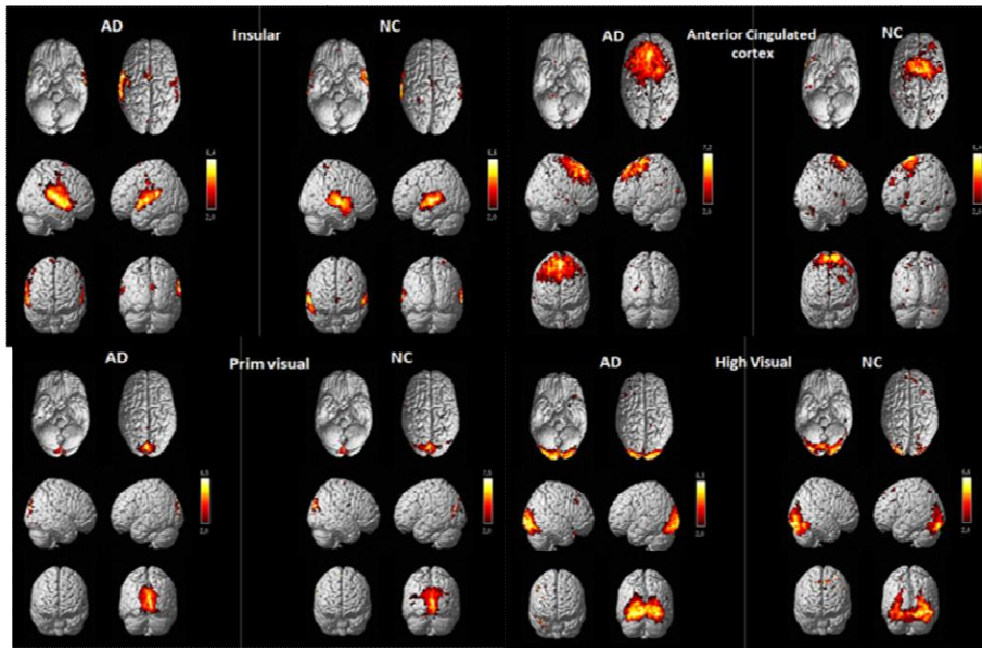


Fig. 3. Salience network and visual network functional activation differences in AD and HC

3.2 Abnormal RSNs in AD Patients

The functional connectivity alterations in abnormal resting-state networks and their brain

regions of AD compared to HC are obtained from two-sample t-test ($P > .03$) is as shown in Figs. 4-5, Table 2 depicts the list of altered functional connectivity sub regions in AD.

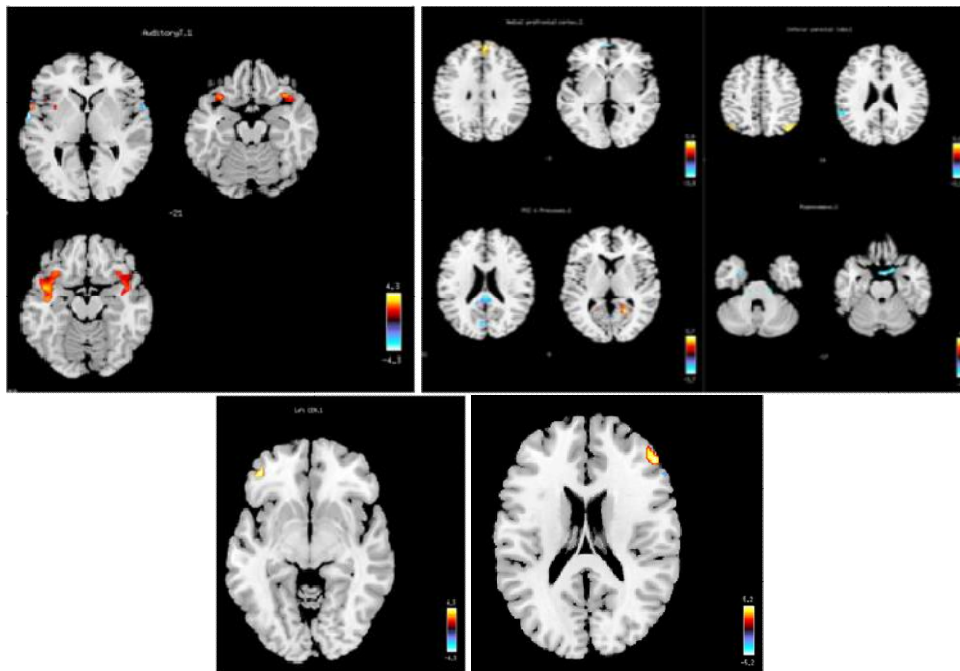


Fig. 4. Abnormal sub-regions in auditory network, default mode network and left & right executive network

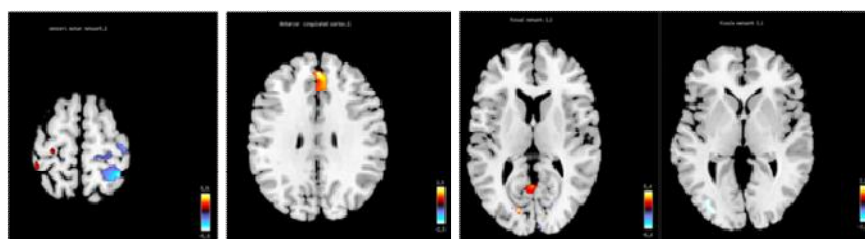


Fig. 5. Abnormal sub-regions in sensory-motor, anterior cingulated cortex & visual network

Table 2. Altered functional connectivity sub regions of AD compared to HC

RSNs	Regions	Sign	Abnormal brain regions	No of Voxels	Peak coordinate
AN	L. Superior temporal gyrus	positive	L middle temporal gyrus	97	-45,-12,-18
	R superior temporal gyrus	positive	R IFG (P Orbitalis)	48	39,24,-21
DMN	Medial prefrontal gyrus	negative	L Superior temporal gyrus	50	-63,-3,0
		positive	R superior medial gyrus	53	6,60,30
	Inferior parietal lobe	negative	L mid orbital gyrus	10	-6, 60,-3
		positive	L angular gyrus	87	-39,-57,63
	PCC & Precunues		R angular gyrus	115	45,-72,63
		negative	L Superior temporal gyrus	21	-63,-45,24
		positive	R Lingual gyrus	51	24,-57,6
Hippocampus		negative	L Calcarine gyrus	45	0,-78,21
		positive	L temporal pole	78	
		negative	L medial temporal pole	78	-27,6,-36
CEN	left	positive	L IFG (P Orbitalis)	24	-42,45,-9
	Right	positive	R IFG (P Triangularis)	66	54,39,18
SN	Anterior cingulated cortex	positive	L Superior medial gyrus	99	3,48,30
	Insular	NC			
SMN		negative	R Superior parietal lobule	51	39,-48,66
VN	High VN	Positive	L Calcarine gyrus	62	-15,-81,9
	Prim VN	negative	Inferior occipital gyrus	62	-33,-87,0

4. DISCUSSION

Resting-state fMRI data of AD vs HC were analyzed using ICA methods in which the decomposition of mixed components represents the actual brain activity and this will be very helpful in clinical treatment. By implementing this method of lower to higher order components extraction, all resting-state network components with both minor and major regions grouping was found. These extracted components were identified and classified using masks with manually specified region of interest. Thus enabling to explore and compare all the regions of the six resting-states networks in both AD and HC revealing the significant group difference. This analysis proved that RSNs of AD patients are

having abnormalities compared to HC. Demonstrating reduced connectivity in RSNs such as in DMN, AN, SMN, and VN which represents the cognitive and sensory networks and increased connectivity in attention networks such as central executive and salience network [34,35].

AN, Auditory network is the part of the temporal lobe that processes auditory information. As suggested the basic auditory capacities in AD should be normal, whereas more significant level of sound-related function should be increasingly damaged [36]. The auditory network includes superior temporal gyrus. Our results shows that increased FC in the left middle temporal gyrus and right inferior frontal gyrus P Orbitalis (IFG P Orbilatis).

Default, salience and central executive networks are highly explored networks in AD. Results of salience and central networks appear to be unstable. Our results is consistent with earlier results, DMN showed decreased connectivity, whereas mean increased connectivity in the central network and in the regions of the salience network of AD [30]. This study shows decreased connectivity in posterior cingulate cortex, precuneus, inferior parietal lobe, medial prefrontal cortex and high functional connectivity in the hippocampus correlating with the previous results [37]. In the sub-regions DMN we observed increased connectivity in the right part of superior medial gyrus, parts of angular gyrus, right lingual gyrus and decreased connectivity in left parts of mid orbital gyrus, superior temporal gyrus and calcarine, the sub-region of hippocampus exhibits increased connectivity in left temporal pole and decreased connectivity in left medial temporal pole.

Default mode networks and salience networks being the part of largest networks are stated to be the early signature in cognitive decline in the AD; the most recent work examined the alterations in AD at two slow frequency bands i.e 0.073-0.198 and 0.01-0.027 [38] and had similar results with displaying decreased connectivity in DMN and increased connectivity in SN along the spectrum too are not variant thus consisting of the strong abnormal regions.

CEN, the central executive network consists of the right and left parts of the dorsolateral prefrontal cortex (DLPFC) and the posterior parietal cortex (PPC). It plays an important role in the maintenance of information in working memory. Our results show increased connectivity in a mean central executive network of AD as reported [30], whereas sub-regions such as left IFG (P orbitalis) and right IFG (P triangularis) exhibits increased connectivity in AD compared to HC.

SN, salience network as suggested by previous studies dynamically controls the default and executive networks; hence we can say that these three networks are functionally correlated [30], SN consists of anterior cingulate cortex and anterior insular, shows increased connectivity and their sub regions of left superior medial gyrus [39,40].

VN, Visual network consists of high and prim visual shows decrease connectivity in AD is allied with visual memory and visuospatial

network [41]. High visual also called as extra striate visual network includes inferior occipital gyrus and prim visual lingual gyrus, calcarine gyrus, and parts of the cerebellum [42]. Our results show reduced functional connectivity in left inferior occipital gyrus and higher connectivity in left calcarine gyrus.

Our study explores on major resting-state network regions, but there are other regions affected due to the disease progression. Distinguishing of these regions by examining the whole brain would result in more significant regions responsible for AD. Second main concern is about the subject's count more number of data would lead to more significant abnormal regions.

5. CONCLUSION

The resting-state fMRI has provided a better understanding of the resting-state networks in AD and normal's. Major RSNs or group of regions that exhibit alterations in spontaneous BOLD fluctuations i.e functional connectivity differences have been identified in AD compared to normals. Parts of temporal gyrus and inferior frontal gyrus along with lingual gyrus, calcarine gyrus, angular gyrus, and temporal pole appear to be abnormal in Alzheimer's during rest. From this study we were able to locate the core regions that would play a major role in the cerebrum damage due to the disease and further these regions would be targeted in performing the classification Alzheimer's with controls.

CONSENT

As per international standard or university standard written participants consent has been collected and preserved by the author(s).

ETHICAL APPROVAL

As per the ADNI protocol, all procedure performed is this study involving human participants were in accordance with the ethical standards of the institutional and/or national research committee and with 1964 Helsinki declaration and its later amendments or comparable ethical standards. More details can be found at adni.loni.usc.edu.

ACKNOWLEDGEMENT

Data collection and sharing for this project was funded by ADNI (National Institute of Health Grants U01 AG024904).

COMPETING INTERESTS

Authors have declared that no competing interests exist.

REFERENCES

1. DeTure MA, Dickson DW. The neuropathological diagnosis of Alzheimer's disease. *Mol Neurodegener.* 2019;14(1): 32.
PMCID: PMC6679484
Available:<http://dx.doi.org/10.1186/s13024-019-0333-5>
2. La Iglesia-Vaya M de, Molina-Mateo J, Jose MSA, Marti-Bonmati L. Brain connections – Resting State fMRI functional connectivity. In: Fountas K, Editor. *Novel Frontiers of Advanced Neuroimaging*; 2013.
3. Lv H, Wang Z, Tong E, Williams LM, Zaharchuk G, Zeineh M, Goldstein-Piekarski AN, Ball TM, Liao C, Wintermark M. Resting-state functional MRI: Everything that non-experts have always wanted to know. *AJNR Am J Neuroradiol.* 2018;39(8):1390–1399.
PMCID: PMC6051935
Available:<http://dx.doi.org/10.3174/ajnr.A5527>
4. Fleisher AS, Sherzai A, Taylor C, Langbaum JBS, Chen K, Buxton RB. Resting-state BOLD networks versus task-associated functional MRI for distinguishing Alzheimer's disease risk groups. *Neuroimage.* 2009;47(4):1678–1690.
PMCID: PMC2722694
Available:<http://dx.doi.org/10.1016/j.neuroimage.2009.06.021>
5. Yao Z, Hu B, Zhao L, Liang C. Analysis of gray matter in AD patients and MCI subjects based Voxel-based morphometry. *Brain Informatics.* 2011;209–217.
Available:http://dx.doi.org/10.1007/978-3-642-23605-1_22
6. Li Y, Wang X, Li Y, Sun Y, Sheng C, Li H, Li X, Yu Y, Chen G, Hu X, Jing B, Wang D, Li K, Jessen F, Xia M, Han Y. Abnormal resting-state functional connectivity strength in mild cognitive impairment and its conversion to Alzheimer's disease. *Neural Plast.* 2016;4680972.
PMCID: PMC4710946
Available:<http://dx.doi.org/10.1155/2016/4680972>
7. Farahani FV, Karwowski W, Lighthall NR. Application of graph theory for identifying connectivity patterns in human brain networks: A systematic review. *Front Neurosci.* 2019;13:585.
PMCID: PMC6582769
Available:<http://dx.doi.org/10.3389/fnins.2019.00585>
8. Bi X-A, Sun Q, Zhao J, Xu Q, Wang L. Non-linear ICA analysis of resting-state fMRI in mild cognitive impairment. *Front Neurosci.* 2018;12:413.
PMCID: PMC6018085
Available:<http://dx.doi.org/10.3389/fnins.2018.00413>
9. Khazaei A, Ebrahimzadeh A, Babajani-Feremi A. Application of advanced machine learning methods on resting-state fMRI network for identification of mild cognitive impairment and Alzheimer's disease. *Brain Imaging Behav.* 2016;10(3): 799–817.
PMID: 26363784
Available:<http://dx.doi.org/10.1007/s11682-015-9448-7>
10. Santana AN, Cifre I, de Santana CN, Montoya P. Using deep learning and resting-state fMRI to classify chronic pain conditions. *Front Neurosci.* 2019;13:1313.
PMCID: PMC6929667
Available:<http://dx.doi.org/10.3389/fnins.2019.01313>
11. Badhwar A, Tam A, Dansereau C, Orban P, Hoffstaedter F, Bellec P. Resting-state network dysfunction in Alzheimer's disease: A systematic review and meta-analysis. *Alzheimers Dement.* 2017;8:73–85.
PMCID: PMC5436069
Available:<http://dx.doi.org/10.1016/j.dadm.2017.03.007>
12. Iraj A, Calhoun VD, Wiseman NM, Davoodi-Bojd E, Avanaki MRN, Haacke EM, Kou Z. The connectivity domain: Analyzing resting-state fMRI data using feature-based data-driven and model-based methods. *Neuroimage.* 2016;134: 494–507.
PMCID: PMC4957565
Available:<http://dx.doi.org/10.1016/j.neuroimage.2016.04.006>
13. Cole DM, Smith SM, Beckmann CF. Advances and pitfalls in the analysis and interpretation of resting-state FMRI data. *Front Syst Neurosci.* 2010;4:8.
PMCID: PMC2854531

- Available:<http://dx.doi.org/10.3389/fnsys.2010.00008>
14. Qureshi MNI, Ryu S, Song J, Lee KH, Lee B. Evaluation of functional decline in Alzheimer's dementia using 3D deep learning and group ICA for rs-fMRI measurements. *Front Aging Neurosci.* 2019;11:8.
PMCID: PMC6378312
Available:<http://dx.doi.org/10.3389/fnagi.2019.00008>
 15. Tian L, Kong Y, Ren J, Varoquaux G, Zang Y, Smith SM. Spatial vs. temporal features in ICA of resting-state fMRI - A quantitative and qualitative investigation in the context of response inhibition. *PLoS One.* 2013;8(6):e66572.
PMCID: PMC3688987
Available:<http://dx.doi.org/10.1371/journal.pone.0066572>
 16. Iraj A, Faghiri A, Lewis N, Fu Z, DeRamus T, Qi S, Rachakonda S, Du Y, Calhoun V. Ultra-high-order ICA: An exploration of highly resolved data-driven representation of intrinsic connectivity networks (sparse ICNs). *International Society for Optics and Photonics.* 2019;1113801.
[Cited 2020 May 28]
 17. Lu J, Zhang H, Hameed NUF, Zhang J, Yuan S, Qiu T, Shen D, Wu J. An automated method for identifying an independent component analysis-based language-related resting-state network in brain tumor subjects for surgical planning. *Sci Rep.* 2017;7(1):13769.
PMCID: PMC5653800
Available:<http://dx.doi.org/10.1038/s41598-017-14248-5>
 18. Griffanti L, Douaud G, Bijsterbosch J, Evangelisti S, Alfaro-Almagro F, Glasser MF, Duff EP, Fitzgibbon S, Westphal R, Carone D, Beckmann CF, Smith SM. Hand classification of fMRI ICA noise components. *Neuroimage.* 2017;154:188–205.
PMCID: PMC5489418
Available:<http://dx.doi.org/10.1016/j.neuroimage.2016.12.036>
 19. Wang Y, Li T-Q. Dimensionality of ICA in resting-state fMRI investigated by feature optimized classification of independent components with SVM. *Front Hum Neurosci.* 2015;9:259.
PMCID: PMC4424860
Available:<http://dx.doi.org/10.3389/fnhum.2015.00259>
 20. Vergun S, Gaggi W, Nair VA, Suhonen JI, Birn RM, Ahmed AS, Meyerand ME, Reuss J, DeYoe EA, Prabhakaran V. Classification and extraction of resting state networks using healthy and epilepsy fMRI data. *Front Neurosci.* 2016;10:440.
PMCID: PMC5037187
Available:<http://dx.doi.org/10.3389/fnins.2016.00440>
 21. Petersen RC, Aisen PS, Beckett LA, Donohue MC, Gamst AC, Harvey DJ, Jack CR Jr, Jagust WJ, Shaw LM, Toga AW, Trojanowski JQ, Weiner MW. Alzheimer's Disease Neuroimaging Initiative (ADNI): Clinical characterization. *Neurology.* 2010;74(3):201–209.
PMCID: PMC2809036
Available:<http://dx.doi.org/10.1212/WNL.0b013e3181cb3e25>
 22. Chao-Gan YAN. Data Processing Assistant for Resting-State fMRI (DPARSF). The R-fMRI Network; 2014.
[Cited 2020 May 28]
Available:<http://rfmri.org/DPARSF>
 23. Erhardt EB, Rachakonda S, Bedrick EJ, Allen EA, Adali T, Calhoun VD. Comparison of multi-subject ICA methods for analysis of fMRI data. *Hum Brain Mapp.* 2011;32(12):2075–2095.
PMCID: PMC3117074
Available:<http://dx.doi.org/10.1002/hbm.21170>
 24. Von dem Hagen EAH, Stoyanova RS, Baron-Cohen S, Calder AJ. Reduced functional connectivity within and between "social" resting state networks in autism spectrum conditions. *Soc Cogn Affect Neurosci.* 2013;8(6):694–701.
PMCID: PMC3739917
Available:<http://dx.doi.org/10.1093/scan/ns053>
 25. Majeed W, Avison MJ. Robust data driven model order estimation for independent component analysis of FMRI data with low contrast to noise. *PLoS One.* 2014;9(4):e94943.
PMCID: PMC4005775
Available:<http://dx.doi.org/10.1371/journal.pone.0094943>
 26. Maldjian JA. WFU Pickatlas.
Available:<http://www.fmri.wfubmc.edu/download.htm>
 27. De Lacy N, Calhoun VD. Dynamic connectivity and the effects of maturation in youth with attention deficit hyperactivity disorder. *Netw Neurosci.* 2019;3(1):195–216.
PMCID: PMC6372020

- Available:http://dx.doi.org/10.1162/netn_a_00063
28. Castellazzi G, Palesi F, Casali S, Vitali P, Sinforiani E, Wheeler-Kingshott CAM, D'Angelo E. A comprehensive assessment of resting state networks: Bidirectional modification of functional integrity in cerebro-cerebellar networks in dementia. *Front Neurosci.* 2014;8:223. PMID: PMC4115623 Available:<http://dx.doi.org/10.3389/fnins.2014.00223>
 29. Rosazza C, Aquino D, D'Incerti L, Cordella R, Andronache A, Zacà D, Bruzzone MG, Tringali G, Minati L. Preoperative mapping of the sensorimotor cortex: Comparative assessment of task-based and resting-state fMRI. *PLoS One.* 2014;9(6):e98860. PMID: PMC4051640 Available:<http://dx.doi.org/10.1371/journal.pone.0098860>
 30. Joo SH, Lim HK, Lee CU. Three large-scale functional brain networks from resting-state functional MRI in subjects with different levels of cognitive impairment. *Psychiatry Investig.* 2016;13(1):1–7. PMID: PMC4701672 Available:<http://dx.doi.org/10.4306/pi.2016.13.1.1>
 31. Moerel M, De Martino F, Formisano E. An anatomical and functional topography of human auditory cortical areas. *Front Neurosci.* 2014;8:225. PMID: PMC4114190 Available:<http://dx.doi.org/10.3389/fnins.2014.00225>
 32. Wang P, Zhou B, Yao H, Zhan Y, Zhang Z, Cui Y, Xu K, Ma J, Wang L, An N, Zhang X, Liu Y, Jiang T. Aberrant intra- and inter-network connectivity architectures in Alzheimer's disease and mild cognitive impairment. *Sci Rep.* 2015;5:14824. PMID: PMC4594099 Available:<http://dx.doi.org/10.1038/srep14824>
 33. Zheng W, Liu X, Song H, Li K, Wang Z. Altered functional connectivity of cognitive-related cerebellar subregions in Alzheimer's disease. *Front Aging Neurosci.* 2017;9:143. PMID: PMC5432635 Available:<http://dx.doi.org/10.3389/fnagi.2017.00143>
 34. Sorg C, Riedl V, Mühlau M, Calhoun VD, Eichele T, Läer L, Drzezga A, Förstl H, Kurz A, Zimmer C, Wohlschläger AM. Selective changes of resting-state networks in individuals at risk for Alzheimer's disease. *Proc Natl Acad Sci USA.* 2007;104(47):18760–18765. PMID: PMC2141850 Available:<http://dx.doi.org/10.1073/pnas.0708803104>
 35. Chand GB, Wu J, Hajjar I, Qiu D. Interactions of the salience network and its subsystems with the default-mode and the central-executive networks in normal aging and mild cognitive impairment. *Brain Connect.* 2017;7(7):401–412. PMID: PMC5647507 Available:<http://dx.doi.org/10.1089/brain.2017.0509>
 36. Lu J, Testa N, Jordan R, Elyan R, Kanekar S, Wang J, Eslinger P, Yang QX, Zhang B, Karunanayaka PR. Functional connectivity between the resting-state olfactory network and the hippocampus in Alzheimer's disease. *Brain Sci.* 2019;9(12). PMID: PMC6955985 Available:<http://dx.doi.org/10.3390/brainsci9120338>
 37. Xue J, Guo H, Gao Y, Wang X, Cui H, Chen Z, Wang B, Xiang J. Altered directed functional connectivity of the hippocampus in mild cognitive impairment and Alzheimer's disease: A resting-state fMRI study. *Front Aging Neurosci.* 2019;11:326. PMID: PMC6905409 Available:<http://dx.doi.org/10.3389/fnagi.2019.00326>
 38. Wang P, Li R, Yu J, Huang Z, Li J. Frequency-dependent brain regional homogeneity alterations in patients with mild cognitive impairment during working memory state relative to resting state. *Front Aging Neurosci.* 2016;8:60. PMID: PMC4805610 Available:<http://dx.doi.org/10.3389/fnagi.2016.00060>
 39. Cera N, Esposito R, Cieri F, Tartaro A. Altered cingulate cortex functional connectivity in normal aging and mild cognitive impairment. *Front Neurosci.* 2019;13:857. PMID: PMC6753224 Available:<http://dx.doi.org/10.3389/fnins.2019.00857>
 40. Liu X, Chen X, Zheng W, Xia M, Han Y, Song H, Li K, He Y, Wang Z. Altered functional connectivity of insular sub regions in Alzheimer's disease. *Front Aging Neurosci.* 2018;10:107. PMID: PMC5905235

- Available:<http://dx.doi.org/10.3389/fnagi.2018.00107>
41. Badhwar A, Tam A, Dansereau C, Orban P, Hoffstaedter F, Bellec P. Resting-state network dysfunction in Alzheimer's disease: A systematic review and meta-analysis Alzheimer's Dement. 2017;8:73–85.
PMCID: PMC5436069
Available:<http://dx.doi.org/10.1016/j.dadm.2017.03.007>
42. Cai S, Chong T, Zhang Y, Li J, von Deneen KM, Ren J, Dong M, Huang L, Alzheimer's disease neuroimaging initiative. altered functional connectivity of fusiform gyrus in subjects with amnesic mild cognitive impairment: A resting-state fMRI study. Front Hum Neurosci. 2015;9:471.
PMCID: PMC4550786
Available:<http://dx.doi.org/10.3389/fnhum.2015.00471>

© 2020 Usha and Dr Suma; This is an Open Access article distributed under the terms of the Creative Commons Attribution License (<http://creativecommons.org/licenses/by/4.0>), which permits unrestricted use, distribution, and reproduction in any medium, provided the original work is properly cited.

Peer-review history:
The peer review history for this paper can be accessed here:
<http://www.sdiarticle4.com/review-history/57122>